



Assessment of Modeling Strategies for Lightly Reinforced Concrete Shear Walls

J. Williams⁽¹⁾, T. Doan⁽²⁾, P. Laursen⁽³⁾, A. Behrouzi⁽⁴⁾

(1) Graduate Student, California Polytechnic State University –San Luis Obispo, CA, USA, jwill107@calpoly.edu

(2) Graduate Student, California Polytechnic State University –San Luis Obispo, CA, USA, tdoan04@calpoly.edu

(3) Professor, California Polytechnic State University –San Luis Obispo, CA, USA, plausen@calpoly.edu

(4) Assistant Professor, California Polytechnic State University –San Luis Obispo, CA, USA, behrouzi@calpoly.edu

Abstract

Pre-1980's non-ductile reinforced concrete wall systems are typically lightly reinforced and lack adequate boundary element detailing, which suggest they are susceptible to brittle, compression-controlled failure modes, and deemed deficient by industry practitioners. Researchers at the California Polytechnic State University [1], San Luis Obispo (Cal Poly), recently tested a slender RC wall with vertical and horizontal reinforcement ratios approaching ACI 318-14 [2] code minimum ($\rho_v = \rho_h = 0.37\%$) and no boundary elements. Results from this wall test will be presented and contrasted with a set of lightly reinforced walls, specimens C1-C3 tested by Lu et al. [3] at the University of Auckland, New Zealand, with higher levels of reinforcement ($\rho_v = 0.53\%$). This paper will examine the Cal Poly and Lu et al. walls by comparing experimental test results. It will also comment on the accuracy of current modelling strategies used by industry practitioners to estimate the strength, stiffness, and ductility of existing lightly reinforced walls. Finally, it will make recommendations for the necessary model calibrations to achieve accurate prediction of the response of the lightly reinforced walls using PERFORM-3D [4], as a refinement of Lowes et al. [5] modeling recommendations for this wall type. The overall goal with this study is to facilitate accurate modeling that will provide detailed understanding of the wall response, and to inform the industry practitioner about the need for retrofitting to meet modern standards.

Keywords: non-ductile concrete walls; experimental behavior; analytical modeling; push-over analysis



1. Introduction

A large number of pre-1980's non-ductile reinforced concrete (RC) structures in California utilizing RC shear walls to resist seismic lateral forces have been identified as deficient by industry practitioners. Poor behavior of lightly reinforced RC walls was observed in many recent earthquakes, including Chile (1985), New Zealand (2010/2011) and Mexico (2017). In order to understand the behavior and failure modes of these walls, the authors compared the performance of lightly reinforced walls from two experimental tests series: Specimens C1-C3 of Lu et al. [3] and the slender reinforced concrete wall of De Sevilla et. al. [1]. Then, these experimental test results were used to draw conclusions on the expected behavior and performance of lightly reinforced concrete walls with low axial loads and no boundary elements. Following this analysis, the accuracy of two wall modelling techniques applied to each of the four walls was evaluated: (a) simplified pushover analyses under the guidance of Priestly [6] and ASCE 41-17 [7] and (b) nonlinear analysis utilizing Perform 3-D under the guidance of Lowes et al. [5]. From these models, recommendations were made in regards to accurate prediction of lightly reinforced concrete shear wall behavior.

2. Experimental Tests of Lightly Reinforced Concrete Walls

The de Sevilla et al. [1] and the Lu et al. [3] experimental test walls are representative of walls that structural engineers have encountered in existing concrete shear wall buildings: low axial and transverse reinforcement ratios, low axial load, and a lack of boundary elements. The geometric and material properties of each wall are shown in Table 1. It is noted that C1-C3 were of the same physical dimensions. The variable shear span to depth ratio was achieved by superimposed moments on C2-C3. All walls were subjected to cyclical loading with the only difference being that W1 underwent an additional high drift monotonic push. A cyclical loading protocol was applied in each scenario and produced similar results shown in Table 2. Unlike expected flexural compression failure (concrete crushing and rebar buckling), each wall failed in flexural tension (rebar fracturing), indicating that industry practitioners may not be pursuing the proper retrofit.

Table 1 – Experimental Wall Parameters

Author	Wall	Length (in)	Height (in)	Thickness (in)	f'_c (ksi)	f_y (ksi)	Reinf. Steel Ratio	Axial Load Ratio	Shear Span to Depth Ratio
de Sevilla et al. [1]	W1	60	153	5	3.80	54.0	0.37%	3.50%	2
Lu et al. [3]	C1	55	110	5.91	5.84	43.5	0.53%	3.50%	2
	C2	55	110	5.91	5.00	43.5	0.53%	3.50%	4
	C3	55	110	5.91	5.25	43.5	0.53%	3.50%	6

1 in = 2.54 cm; 1 ksi = 6.89 MPa

Table 2– Experimental Wall Results

Author	Wall	Applied M_{max} (k-ft)	Applied F_{max} (k)	First Cracking (% drift)	Rebar Buckling (% drift)	Concrete Crushing (% drift)	Rebar Fracture (% drift)	Drift Capacity (%)	Failure Mode
de Sevilla et al. [1]	W1	268	21	0.20%	NA	NA	1.67%	1.67%	FT
Lu et al. [3]	C1	486	39	0.20%	1.50%	2.00%	2.50%	2.50%	FT
	C2	499	20	0.06%	1.50%	2.00%	2.50%	2.50%	FT
	C3	475	13	0.16%	1.50%	2.00%	2.50%	2.50%	FT

1 k = 4.45 KN; 1 ft = 30.48 cm; FT = flexural tension; NA = minimal observations of the state achieved

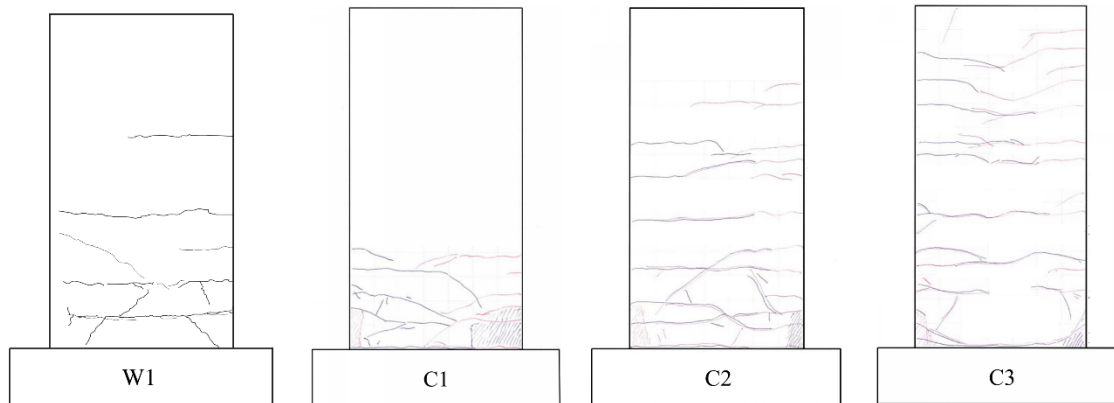


Fig. 1 – Observed Crack Patterns in de Sevilla et al. [1] and Lu et al. [3]

The observed crack pattern was a strong indication of flexural behavior and failure (Fig. 1). Large, main flexural cracks formed at the base of each wall, extending up the wall height in relation to the shear span to depth ratio, respectively. Although C2 and C3 had similar applied loads as C1, in terms of base moment, they experienced more significant cracking due to additional applied moment. However, concrete crushing was limited in all test due to flexural cracking and rebar yielding, which did not compromise the concrete compression zones in reverse cycles. The wide spacing of the flexural cracks caused rebar strain concentration in these cracks and ultimately resulted in failure of the rebar in the base crack. Effectively, the tensile strength of the concrete surrounding the rebars could only be overcome by the rebar in few distinct locations.

The global hysteresis plots for the walls revealed the overall behavior in terms of the strength, stiffness degradation and energy loss (Fig. 2). The base moments were normalized by the nominal flexural strength of each wall. All walls were subjected to cyclical excursions twice to each desired drift level. The differences in their peak loads and corresponding drifts was due to walls C1-C3 being subjected to higher base moments than wall W1, attributable to a higher reinforcement ratio. Wall C2-C3 were subjected to an additional superimposed moment to mimic a multi-story wall, resulting in higher shear span ratios and propagation of flexural cracks further up the height of the wall.

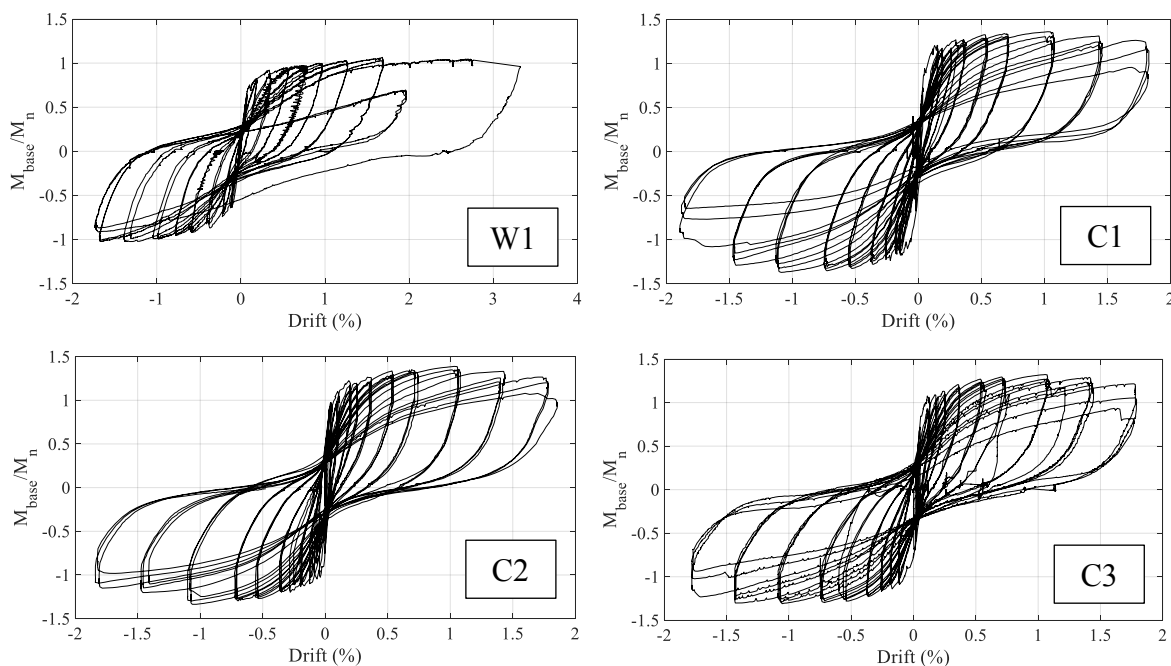


Fig. 2 – Experimental Global Hysteresis Results

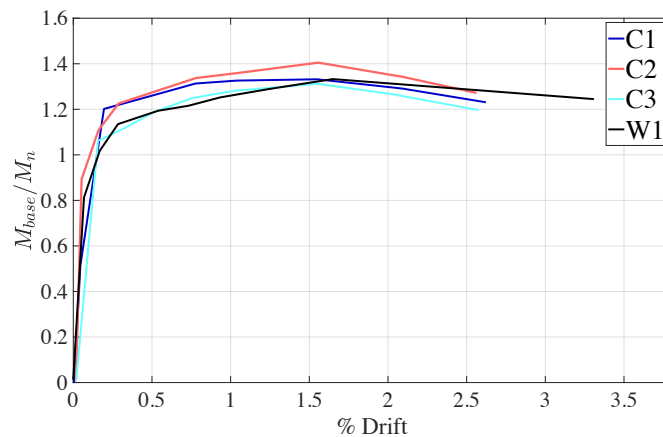


Fig. 3 - Experimental Pushover Results

The drift increments for walls C1-C3 were more evenly applied than those of W1. W1 was cycled to a peak drift beyond that of the C1-C3 walls. All walls showed similar hysteretic behavior and minimal base sliding. Experimental peak envelopes curves were generated from the backbone of the hysteretic loops for the push direction (Fig. 3). The observed crack pattern and global hysteresis for each wall test led the authors to believe that these tests show comparable response and may be used for further investigation of the behavior of lightly reinforced walls.

3. Modeling Implementation

Accurate concrete shear wall modelling is of interest to structural engineering practitioners who to estimate the strength, stiffness, and ductility of existing lightly reinforced concrete shear walls prior to retrofitting. To explore popular modeling technique for lightly reinforced concrete shear walls with low axial load, the walls were modeled using two simplified pushover techniques and a finite element based cyclic analysis.

3.1 Pushover Analysis with Priestley (2017)

The simplified pushover analysis procedure by Priestley [6] proposes direct displacement-based design as an alternative to the more commonly used force-based design. This method requires a moment-curvature analysis with a plastic hinge implementation to produce the force-displacement curve.

Moment-curvature analysis (Fig. 4) was executed using XTRACT [8], a sectional analysis software that allows the user to input material properties and material models. The stress-strain relationship of the concrete was defined using an unconfined Mander [9] model, with the ultimate strain taken as 0.005. The steel reinforcement was defined using a bilinearization with strain hardening model. The moment-curvature was idealized as a bilinear relationship with two limit states, nominal capacity (ϕ_y , M_n) and ultimate capacity (ϕ_u , M_u).

At peak displacement the curvature was considered constant and equal to the maximum value over the calculated plastic hinge length. The plastic hinge length accounts for additional displacement resulting from strain penetration into the foundation.

The force-displacement relationship (Fig. 5) consists of four limit states from the moment-curvature analysis: concrete cracking (Δ_{cr} , F_{cr}), first global yield (Δ'_y , F_y), nominal capacity (Δ_y , F_n) and ultimate capacity (Δ_u , F_u). The latter two states depend on the plastic hinge length and peak concrete strains of 0.003 and 0.005, respectively. The results of this method produced a nearly bilinear force displacement relationship with an initial and final stiffness.

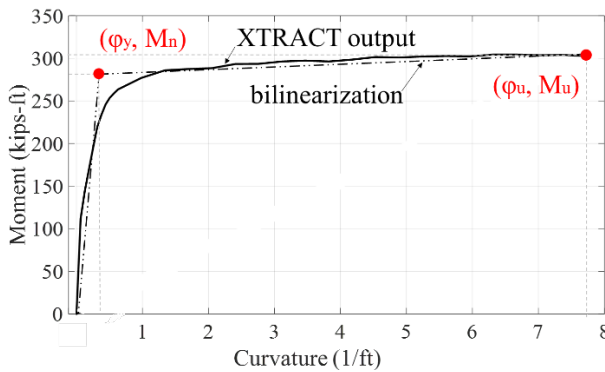


Fig. 4 – XTRACT Moment-Curvature Relationship

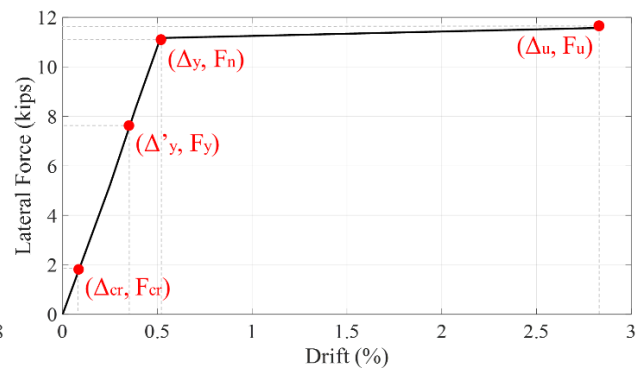


Fig. 5 – Priestley Force-Displacement Relationship

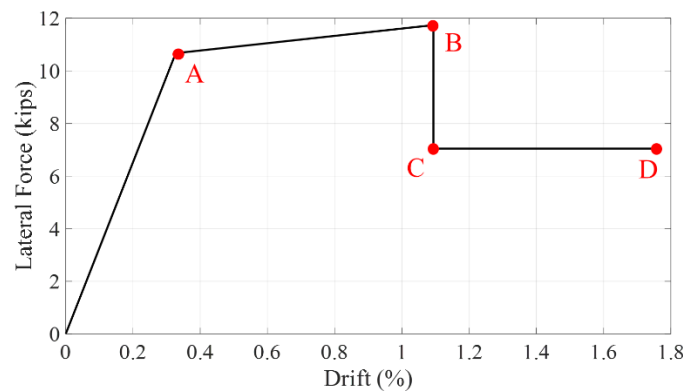


Fig. 6 – ASCE 41-17 Force-Displacement Relationship for Wall C3

3.2 Pushover Analysis with ASCE 41-17

The ASCE 41-17 [7], Seismic Evaluation and Retrofit of Existing Buildings, is the United States' governing code used in the structural engineering industry to estimate the strength of existing structural systems. ASCE 41-17 defines concrete structural walls as deformation-controlled, with the acceptable displacement criteria at expected strength levels defined in Table 10-19 for low axial and low reinforcement ratio concrete shear walls. Plastic hinge rotations are defined for four states: effective yield (A), ultimate strength (B), initial loss of resistance (C), and final loss of resistance (D) shown in Figure 6. Per recommendations from industry partners, the plastic hinge length was defined by $l_w/2$ where l_w is the wall length, as opposed to that proposed in ASCE 41-17.

Initial loading of the component leads to point A (expected strength), followed by an increase in resistance due to strain hardening from point A to point B. The initial loss of resistance (C) leads to reduced resistance, and eventual failure at point D (considered the wall ultimate drift capacity herein). The expected strength (A) was calculated in accordance with ACI 318 [2] with expected material strengths and a strength reduction factor of 1.0. Fig. 6 shows the force-displacement relationship developed for Wall C3.

3.3 Cyclic Load Analysis with PERFORM-3D

To relate to the modeling method described in this section, the reader is expected to have a basic understanding of PERFORM-3D. As a starting point to model a wall system with PERFORM-3D that can adequately capture stiffness, energy dissipation, strength, and material degradation per experimental data, Lowes et al. [5] recommendations were implemented.



The wall cross sections were modeled using geometric and material properties from Table 1. Concrete and steel material models were generated following Lowes et al. guidelines. To assess the performance of walls under cyclic loading, the nonlinear material model “YULRX” was used to define the responses of concrete and steel fibers. This trilinear model depicts uncracked, cracked, and “yielding” behavior of reinforced concrete. Strength deterioration due to cyclic loading is implicitly included in the “YULRX” envelope, and specified stress (F^*) and strain (D^*) values define the tension and compression response (Table 3). Lowes et al. [3] recommends the use of the shear wall element, non-buckling inelastic steel material, and inelastic unconfined concrete material for modeling.

In order to create a PERFORM-3D model that captures the specific behavior of lightly reinforced concrete shear walls, the consequences of meshing and unloading and reloading stiffness factors were explored. The meshing was expected to strongly influence the wall strength and displacement capacity, while the unloading/reloading stiffness factors strongly affect the hysteretic energy dissipation. It is noted that the model results presented in this section did not capture the onset of strength degradation clearly (concrete crushing and rebar fracture). These aspects will be investigated in future analyses. Table 3 shows the PERFORM-3D model input recommendations and are a combination of guidelines from Lowes et al. and the authors’ findings described in further detail in the following sections.

3.3.1 Meshing

Meshing consists in dividing the wall into multiple elements along both the length and the height of the wall in order to capture the overall experimental behavior adequately. Meshing for the model of C1, C2, C3 and W1 was done with careful consideration of the wall cross sections. The cross sections were divided horizontally into 7 nearly equal sized elements. The horizontal meshing remained constant and was dictated by concrete geometry and rebar location. Three vertical mesh sizes were implemented for each wall; C1-C3 was divided into 4, 7, and 10 elements vertically while W1 was similarly divided into 3, 6, and 9 elements vertically (see Fig. 7(a)).

Table 3 – PERFORM-3D Recommendations

Method	Factor	Numerical Input
Lowes et al. [5] Recommendations	Energy Dissipation Factors	YULRX: Y=1.0, U=0.4, L=0.4, R=0.1, X=0.1
	Unconfined Concrete Material Model	DU=0.002, DX=0.025, DL= 0.00202, DR=0.01, FR/FU=0.001
	Steel Reinforcement Material Model	DU=0.05, DX=0.205, DL= 0.18, DR=0.19, FR/FU=0.01
Authors' Recommendations	Vertical Meshing	4 - 10 elements
	Stiffness Factors	SF = 0

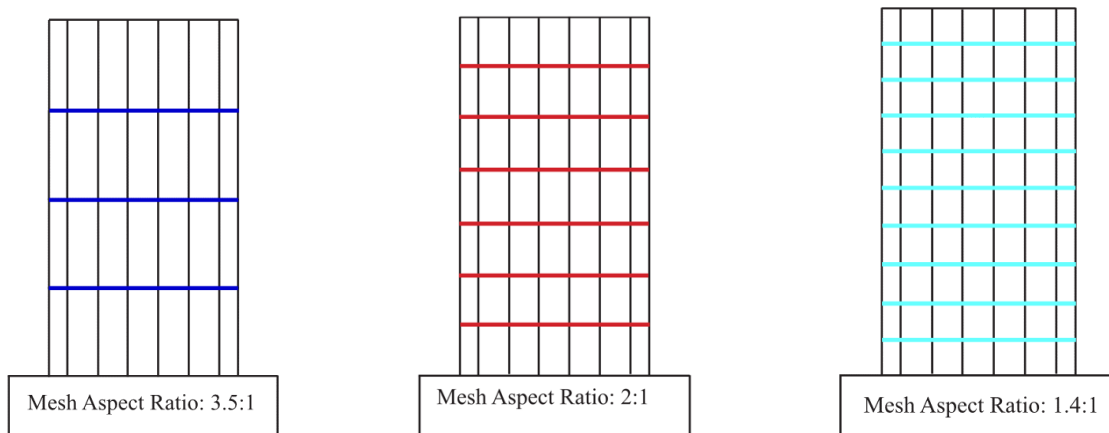


Fig. 7(a) – PERFORM-3D Wall Response to Vertical Meshing

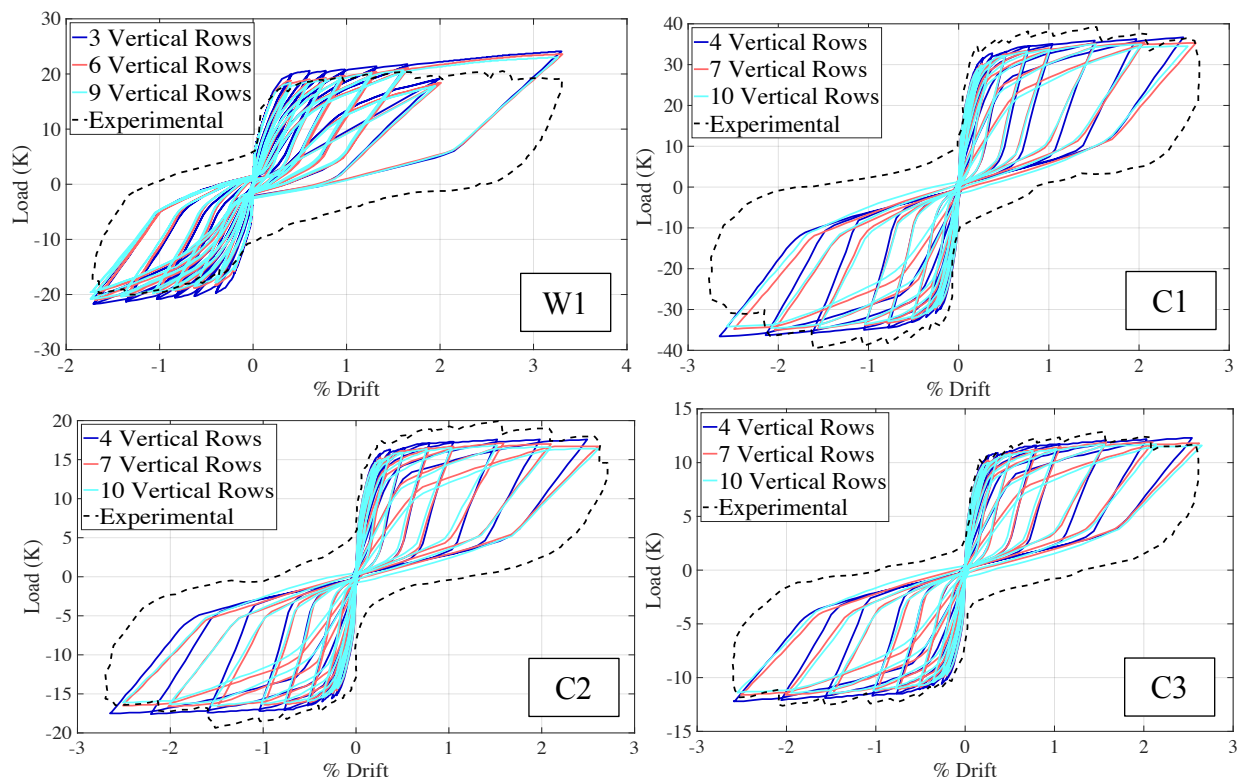


Fig. 7(b) – PERFORM-3D Wall Response to Vertical Meshing (SF = 0)

Fig. 7(b) shows the model cyclical response and the envelope of the experimental results. Coarser vertical meshing resulted in slightly higher resisting load, however this effect is minor for the meshes investigated. The finer meshes better captured the initial stiffness and strength degradation for the C walls. Having more vertical elements resulted in slightly less hysteretic energy dissipation in the system, and the hysteretic curves appear to be slightly more pinched than that of analysis with fewer vertical elements. The strength of W1 appears slightly overestimated while the strength of C1-C3 appear slightly underestimated, irrespective of meshing. It is noted that comparison of strength prediction to experimental wall strength should be made with consideration of the uncertainty in material properties and experimental measurements. The lower moment gradients in walls C2 and C3 (in comparison to C1) would indicate that fewer elements are required vertically to accurately capture the response. This is not clearly expressed in these analyses. Considering initial wall stiffness and ability to capture strength degradation, there is a slight preference of the



most detailed mesh. Clearly, as stated above, the vertical size of the bottom row of elements influences the wall displacement capacity. At this stage of the research, it is considered reasonable to implement between 4 and 10 elements vertically. A mesh with 10 elements better captured strength degradation and is also expected to provide the most conservative predictions of the drift capacity.

3.3.2 Unloading/Reloading Stiffness Factors

PERFORM-3D allows for specification of the extent to which unloading and/or reloading stiffness deviates from a material that is elastic-perfectly-plastic with linear strain hardening. Three different stiffness factors, $-1, 0$, and 1 , were implemented to explore the shape of the hysteresis curves and the ability to capture material stiffness loss and the energy dissipated under cyclic loading. The unloading/reloading stiffness factor is defined in relation to the ratio of the energy dissipated during a stress-strain cycle for the material with stiffness loss, to the energy dissipated without stiffness loss. Meshing with 6 and 7 vertical rows was implemented for W1 and C1-C3, respectively.

The predicted response for the stiffness factors selected were compared to the experimental envelopes at 2% drift for C1-C3, and 1.65% drift for W1, as shown in Fig. 8. The results showed that the resistance at peak displacements was unaffected by the variation of stiffness factors. The only changing aspect was the amount of energy captured. A higher stiffness factor resulted in a system with more strain energy dissipation and more accurate representation of the unloading stiffness. Clearly, these factors altered the shape of the overall hysteresis envelope more drastically than the variations of vertical meshing. A stiffness factor of zero, however, more consistently captured the shape of the experimental hysteresis curves and is retained herein.

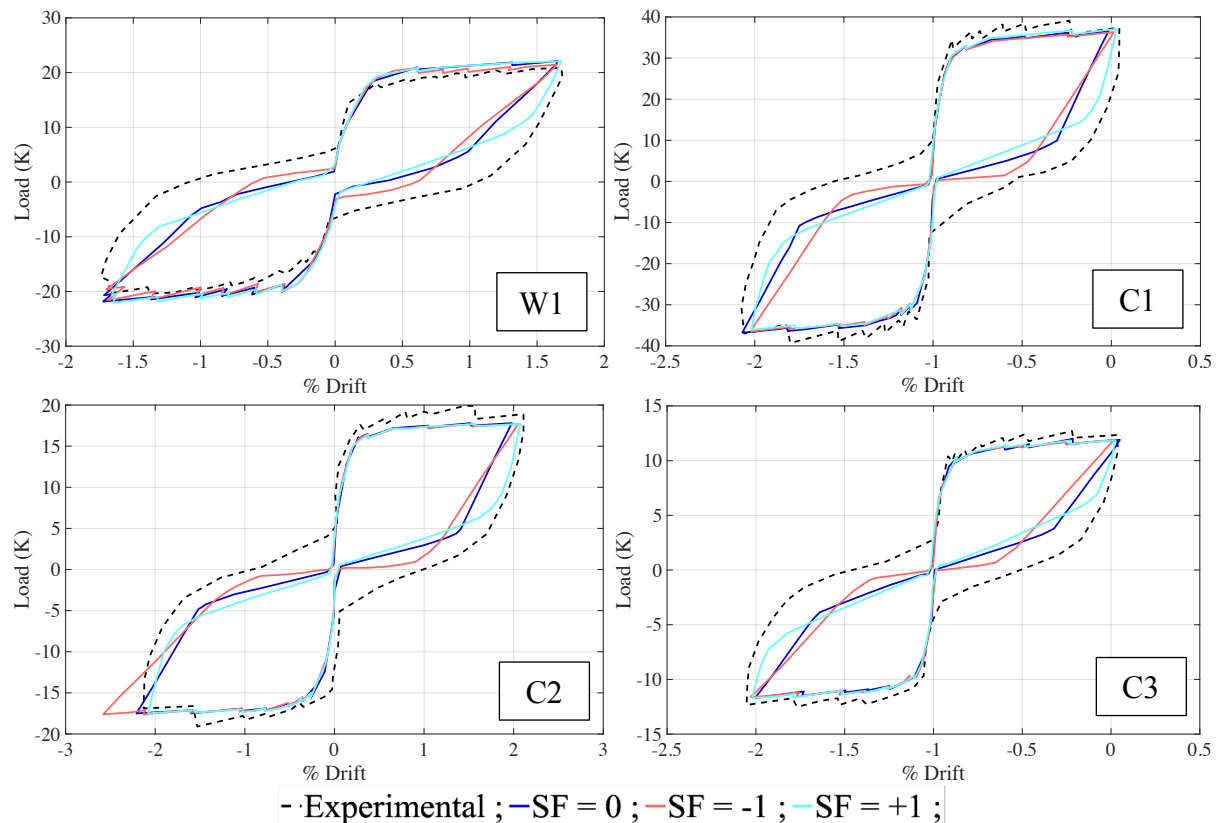


Fig. 8 – PERFORM-3D Wall Response to Stiffness Factors



3.4 Plastic Hinge Length Comparison

Lumped plasticity models rely on estimating a plastic hinge length (L_p). Variability in plastic hinge length definition, limit concrete and steel strains and calculation procedures are indicative of how well the wall behavior is being captured. The Priestley plastic hinge length is defined by k , a ratio of ultimate to yield rebar strain, L_c , the length from the critical section to the point of contraflexure in the wall, and L_{sp} , the strain penetration length into the foundation. ASCE 41-17 gives the plastic hinge length in relation to the wall height. However a practitioner survey suggest that current practice is to assume a plastic hinge length of about half of the wall length: $L_w/2$. The PERFORM-3D effective (equivalent) plastic hinge length is related to the cross-section meshing, particularly the height of the lowest row of elements. Table 4 presents the plastic hinge length estimates as described above and can be used to inform the PERFORM-3D model meshing.

Table 4 – Plastic Hinge Length

Method	Definition (in)	C1 (in)	C2 (in)	C3 (in)	W1 (in)
Priestley [6]	$L_p = kL_c + L_{sp}$	16.87	25.67	34.47	21.28
ASCE 41-17 [7]*	$L_p = L_w/2$	30.00	27.50	27.50	27.50
PERFORM-3D**	height of first element row	27.50	27.50	27.50	38.25

*industry recommendation; **4 element vertical mesh

4. Modeling Comments

This section summarizes the modeling outcomes and provides indication of levels of accuracy that can be achieved in behavioral modeling of lightly reinforced, flexure dominated concrete shear walls. Table 6 includes average ratios of the analytical to experimental values for walls W1 and C1-C3. It is noted that initial stiffness (secant stiffness from origin to (Δ_y, F_n)) and drift ratios for Priestley and ASCE 41-17 are based solely on walls W1 and C1 because the C2 and C3 experiments lack physical representation of the flexibility of the simulated wall height. To qualitatively convey the results, Table 6 and Figure 9 are available.

Table 5 – Quantitative Modeling Accuracy, average values**

Method	Initial Stiffness	Nominal Strength	Yield Drift	Yield Moment	Peak Drift	Peak Moment	Legend (deviation from experiment)	
Priestley [6]	1.10	0.97	1.16	0.87	0.52	0.93	>1	overestimate
ASCE 41-17 [7]	2.00	0.93	0.83	1.11	0.46	0.93	<1	underestimate
PERFORM-3D*	1.23	0.97	1.36	1.05	N/A	1.01	1	accurate

*) 6 and 7 element vertical meshing, **) Initial stiffness and drift values for Priestley and ASCE 41-17 based on W1 and C1 only

Table 6 – Qualitative Modeling Accuracy

Method	Stiffness	Strength	Ductility	Cyclic Degradation	Energy Dissipation	Legend	
Priestley [6]	-	✓	-	N/A	N/A	+	overestimate
ASCE 41-17 [7]	+	✓	-	N/A	N/A	-	underestimate
PERFORM-3D	✓	✓	N/A	-	-	✓	accurate

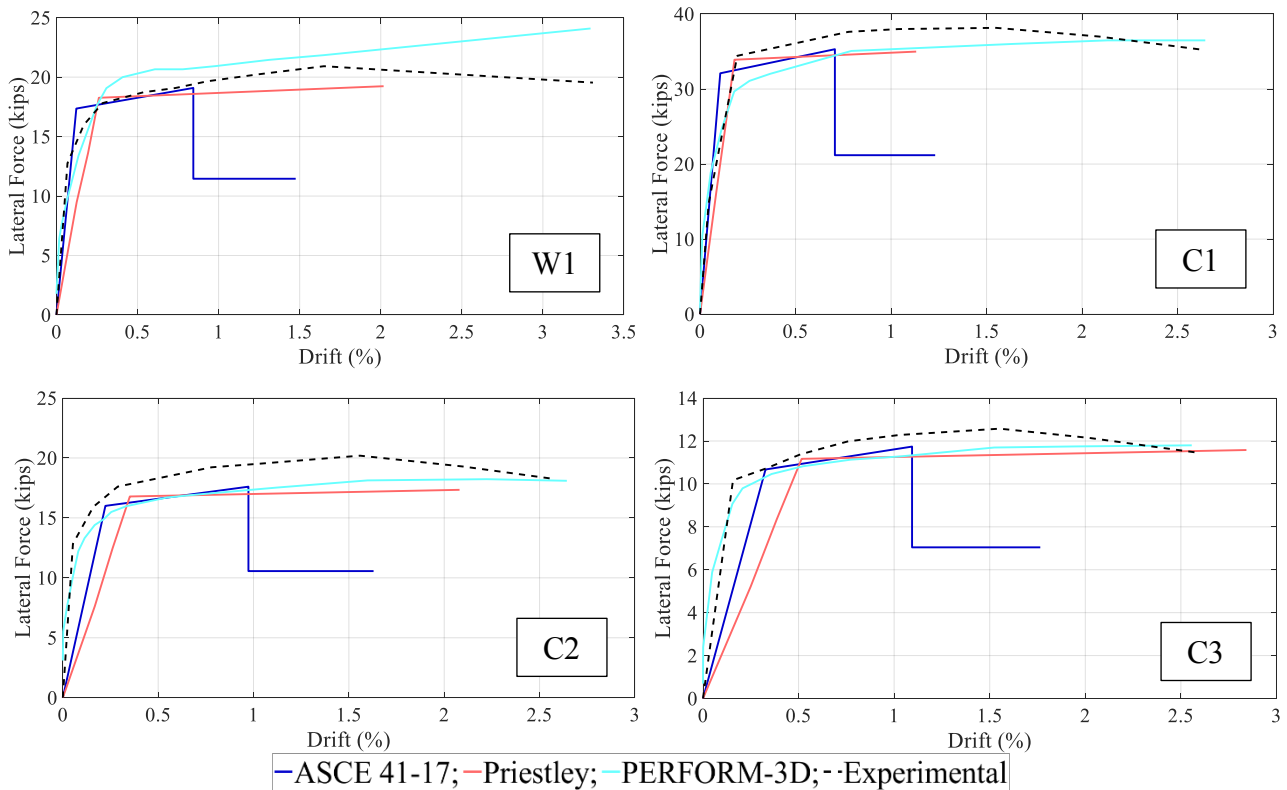


Fig. 9 – Pushover Curve Modeling Comparison

4.1 Priestley Pushover Analysis

Pushover analyses following Priestley [6] guidelines produced a bilinearization that mimicked the curvilinear pushover behavior. Looking at W1 and C1 results in Fig. 9, reveals that the initial stiffness and wall resistance are reasonably well captured. The ultimate drift capacity for W1 is slightly underestimated (2% vs 2.5% for the experiment). This method predicts concrete compression failure while the experiments showed failure due to rupture of the rebar. Although a relatively straightforward approach to creating a force-displacement relationship, a phenomenologically based method like this one would require a calibration (limit concrete and steel strains) with respect to the wall type investigated herein in order to pass plan check approval.

4.2 ASCE 41-17 Pushover Analysis

ASCE 41-17 overestimates the initial stiffness, provides accurate estimate of the wall strength, significantly underestimates the wall drift capacity, and significantly overestimates the wall strength deterioration. The initial stiffness relies on the effective stiffness assumed at nominal strength (taken here as $0.35EI$) and should be assumed much lower, perhaps of the order of $0.2EI$. The wall drift capacity is underestimated for multiple reasons. Notably, that ASCE 41-17 serves as an assessment tool, thus conservative of nature, and that the failure mode considered in the model probably is flexural compression and not flexural tension as was observed in the wall tests. Using ASCE 41-17 would lead industry practitioners to fail predicting the correct failure mode of these walls, thus possibly pursuing a flawed retrofit scheme.



4.3 Cyclic Load Analysis with PERFORM-3D

Following the modeling recommendations herein consistently produced good estimates of wall performance in terms of initial stiffness, yield force and drift, and strength. Calibration of stiffness factors and meshing led to relatively accurate hysteretic performance. Strength degradation onset was captured for C1-C3, but not for W1. Further, the PERFORM-3D models were not equipped to capture the ultimate drift capacity. This must be addressed by investigating concrete and rebar strain as the model is cycled through the numerous displacement excursions. Correlation must be made between experimental and model strain to potentially adjust the material models and meshing of the wall. The wall ultimate drift capacity can then be determined as the drift corresponding to critical strain events related to concrete crushing and rebar fracture.

5. Future Work

5.1 Modeling Strategies

Clearly, PERFORM-3D captures most aspects of wall behavior well using the present modeling recommendations. With further modeling adjustments, the authors intend to improve to the modeling accuracy through the following actions. These will be reflected in a document currently under preparation [10].

- *Implement modeling with strain limit states:* By monitoring critical strain it is expected to be able to capture both flexural compression and flexural tension failure. Previous modeling analyzed a displacement-controlled cyclic load test, with limited success in capturing cyclic degradation.
- *Explore the effect of including concrete tension strength:* The flexural tension failure mode found for all walls indicates that the material model possibly should include this effect.

5.2 Experimental Testing

In addition to investigating modeling strategies, the authors disseminated an industry survey to collect information on typical wall geometry, analysis methods, and viable retrofit solutions associated with flexure dominated, lightly reinforced concrete shear walls. This information will be used to determine the geometry and material parameters for a baseline wall to be designed, built, and tested at Cal Poly. Subsequently, it is anticipated to repair, retrofit and retest the wall.

6. Conclusions

The behavior and performance of slender lightly reinforced concrete walls were investigated with pushover analyses based on lumped plasticity modeling by Priestley [6] and ASCE 41-17 [7], and with PERFORM-3D finite element modeling. It was found that Priestley and ASCE-41 accurately predicted the strength, Priestley accurately predicted the initial stiffness, but the both Priestley and ASCE 41-17 were limited in their capabilities to capture the wall ultimate drift capacity. With appropriate modeling in PERFORM-3D, the authors succeeded in capturing most aspects of real wall behavior. It is expected that the wall ultimate drift capacity can be determined from the PERFORM-3D models by monitoring critical concrete and rebar strain during cycling of the model. The FE wall analysis technique presented herein in combination with the above-mentioned industry survey and further experimental evidence will contribute to the industry knowledgebase. It will allow structural engineers to assess, analyze and retrofit existing deficient buildings with non-ductile reinforced concrete walls.

7. Acknowledgements

Funding for this project was provided by the Cal Poly Research, Scholarly, and Creative Activities grant program as well as the Department of Architectural Engineering. External funding was provided by the



Structural Engineering Foundation. The authors would also like to specifically acknowledge the considerable contributions of industry advisor Garrett Hagen.

9. References

- [1] De Sevilla et al., “Feasibility of a Fiber Reinforced Polymer Retrofit for Non-Ductile Concrete Walls,” *2019 SEAOC Convention Proceedings*, 2019.
- [2] ACI 318-14, Building Code Requirements for Structural Concrete, American Concrete Institute, 2014.
- [3] Lu, Yiqiu, et.al., “Cyclic Testing of Reinforced Concrete Walls with Distributed Minimum Vertical Reinforcement,” *Journal of Structural Engineering*, vol. 143, no. 5, 2017.
- [4] Computers and Structures, Inc. (CSI), “User Guide PERFORM-3DTM: Nonlinear Analysis and Performance Assessment for 3D Structures, CSI, v. 5, June 2011.
- [5] Lowes, Laura & Baker, Carson, “Recommendations for Modeling the Nonlinear Response of Slender Reinforced Concrete Walls Using PERFORM-3D”, *2016 SEAOC Convention Proceedings*, 2016.
- [6] Priestley, M. J. N., et. al., “Displacement-Based Seismic Design of Structures,” EUCENTRE, 2017.
- [7] ASCE 41-17, Seismic Evaluation and Retrofit of Existing Buildings, American Society of Civil Engineers, 2017.
- [8] Chadwell, C.B., and R.A. Imbsen, “XTRACT: A Tool for Axial Force-Ultimate Curvature Interactions,” *Proceedings for 2004 ASCE-SEI Structures Congress*, 2004.
- [9] Mander, J.B., et. al., “Theoretical Stress-Strain Model for Confined Concrete.” *Journal of Structural Engineering*, 1984.
- [10] Williams, Jenna & Doan, Tracy (2020, in preparation). Investigation of Flexure Dominated Lightly Reinforced Concrete Shear Walls Through Surveying, Modeling, and Testing. *Digital Commons*.